

# Energy-Aware Design of Multilayer Core Networks [Invited]

Arsalan Ahmad, Andrea Bianco, Edoardo Bonetto, Luca Chiaraviglio, Filip Idzikowski

**Abstract**—We consider the power-efficient design of an Internet Protocol (IP)-over-Wavelength Division Multiplexing (WDM) network, tackling the problem of installing optical and IP layer equipment to satisfy traffic requirements. We take into account routing constraints and consider a comprehensive set of realistic scenarios defined by a network topology, traffic matrix, and power consumption values of network devices in both layers. Furthermore, besides defining and solving an optimal Mixed-Integer Linear Programming (MILP) model, we propose an efficient heuristic to solve the problem up to medium-sized networks. The proposed heuristic requires at most 30% of additional power w.r.t. the optimal solution, but with a significantly reduced complexity. We show that the largest power consumption is due to line cards and routers rather than WDM equipment. Furthermore, we find that Multi-Path Routing (MPR) reduces the network power consumption w.r.t. Single-Path Routing (SPR), but not significantly. Finally, we show that a two-step design procedure, in which power is separately minimized in each layer (i.e., IP and WDM layers), can find results with a total power consumption comparable to the one achieved by a more complex joint multilayer design procedure.

**Index Terms**—Energy awareness; Multi-Layer core networks; Network design; Optical networks.

## I. INTRODUCTION

Network equipment is estimated to consume a significant and increasing share of worldwide power consumption [1]. As a consequence, the research community is devoting significant efforts on devising power-efficient solutions for telecommunication networks [2], [3], [4], [5], and several research projects address the issue of energy efficient networking.

Although power consumption of access networks is today largely dominant in operator's telecommunication networks, core segments show the largest increase in power consumption [6] and are expected to become a major source of power consumption in future networks. Today's network core segments are usually implemented using two separate layers: an optical layer exploiting the WDM technology and an electrical layer taking care of transporting IP traffic. In multilayer core networks, switching/routing elements are high-performance devices easily consuming tens of kilowatts [7] due to the high data rates they sustain and to the need for cooling systems. Furthermore, optical links covering Long Haul (LH) distances require power-hungry optical amplifiers.

In this paper we consider the network design of an IP-over-WDM multilayer network. In Fig. 1, a model of the network architecture is shown. The IP layer is composed of IP routers in which line cards are located. IP routers are

A. Ahmad, A. Bianco, and E. Bonetto are with the Department of Electronics and Telecommunications, Politecnico di Torino, Torino, Italy (e-mail: {firstname.lastname}@polito.it).

L. Chiaraviglio is with DIET Department, University of Rome - La Sapienza, Rome, Italy (e-mail: luca.chiaraviglio@diet.uniroma1.it)

F. Idzikowski is with Technische Universität Berlin, TKN, Berlin, Germany (e-mail: filip.idzikowski@tu-berlin.de).

©2013 Optical Society of America

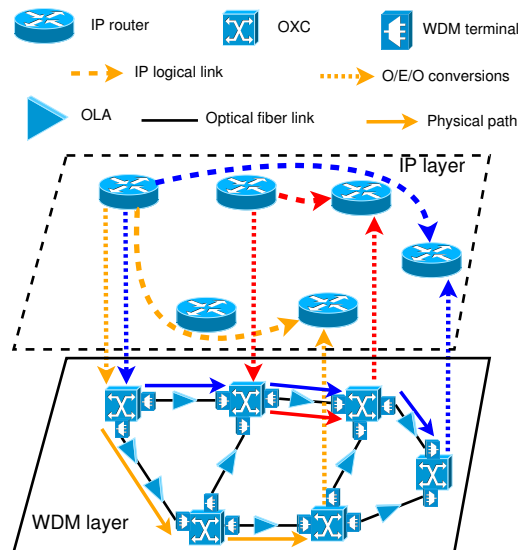


Fig. 1. (Color online) IP-over-WDM multilayer core network architecture.

devoted to IP traffic switching. Line cards, responsible for the Optical-Electrical-Optical (OEO) conversions, originate and terminate the IP logical links (bundles of lightpaths<sup>1</sup>) that are in charge of transporting the IP traffic. The WDM layer is realized by optical fiber links, which include Optical Line Amplifiers (OLAs) and WDM terminals, and Optical Cross-Connects (OXCs), which route the lightpaths over the different fiber links. In this context, we optimize the power consumption not only of the IP layer, by defining which routers and line cards to install and how to route the traffic over the set of IP logical links, but also of the WDM layer where IP logical links are set up.

In the literature, the topic of power-aware design of optical backbone networks has been investigated in different works, e.g., [8], [9], [10]. Most of previous contributions focus on Multi-Commodity Flow (MCF) [11] modeling, i.e., the transportation problem where multiple commodities (traffic demands) need to be routed over a network with limited capacity. MCF (corresponding to MPR in our work) assumes that a traffic demand can be split over different paths, an assumption that often cannot be applied in telecommunication networks because routing protocols are usually constrained to SPR, i.e., the traffic demand between a source and a target node is entirely routed over the same IP path. On the contrary, in this paper we design optical networks considering the constraints imposed by routing policies. We formulate the design model as an optimization problem with SPR constraint, explicitly targeting power minimization. We wish

<sup>1</sup>A lightpath is a WDM channel which spans one or multiple fiber links.

to verify the intuition that using MPR brings substantial power benefits over SPR at the network design stage.

We extend our previous works [12], [13] by: i) comparing the optimal solution with a new algorithm that can scale up to medium-sized networks (i.e., up to hundreds of nodes); ii) evaluating our solution over several research and operator networks; iii) considering the impact of solving the problem on each layer either separately or jointly. Our main findings are: i) the proposed heuristic algorithm provides solutions close to the optimal ones; ii) MPR only slightly reduces the network power consumption; iii) similar results are obtained by solving the design jointly or independently per layer.

The paper is organized as follows: Section II reviews the related work. Section III details the problem formulation. Section IV describes the proposed algorithm. The description of adopted networks and power consumption models is provided in Section V. Results are presented and discussed in Section VI. Finally, Section VII presents conclusions and future work.

## II. RELATED WORK

We provide an overview of the works focusing on the green network design. While the term “design” may be used in different contexts, the main criterion for us to classify a method as a “network design method” is the lack of constraints on the number of installed devices in the network. This means that the methods determining the set of devices that can be put into a standby mode are out of scope of this survey. We look at the methods making decisions about which routers, line cards, transponders, OXCs, OLAs, fibers, etc. to install in the network. The works explicitly focusing on the design of the IP layer (e.g., [14]) or WDM layer (e.g., [15]) are left aside of this survey. We start with the works that cover all types of the devices (from the installation of fibers up to installation of line cards), and then look at the works not determining the fibers to install.

### A. IP and WDM Layers With Fiber Installation

The problem of designing a protected backbone network is formulated as a MILP in [16]. It includes IP routing (both single- and multi-path), Logical Topology (LT) design, realization of lightpaths in the physical layer, and installation of fibers. The problem is solved on a network with 20 nodes and 29 physical links using realistic input data. No heuristic approaches are proposed.

Shen and Tucker present a network design model in [9]. Their MILP minimizes power consumption of the network, and determines the number of fibers installed on a physical link, established lightpaths and their routing, as well as split routing of IP traffic. Differently from our work, various router configurations are not considered. An optimal solution is achieved for small networks with fibers accommodating 16 wavelengths. Heuristic approaches called direct bypass and multi-hop bypass are proposed. The power-minimized network is compared with the network designed with the objective of cost minimization (in \$). No single-path IP routing is considered in the MILP. The multi-hop bypass heuristic seems to be based on the shortest-path routing (indicated also in [17]).

Design of energy-efficient Mixed Line Rate (MLR) networks is tackled in [18]. The authors formulate three MILPs

for a transparent, translucent and opaque IP-over-WDM networks. The number of fibers on a physical link, established lightpaths (taking physical layer constraints into account) and multi-path routing of IP traffic over the virtual topology are kept as variables. The power consumption of basic nodes (IP routers and OXCs) is not included in the objective function, but the devices to be installed can be determined out of the variables mentioned above. No heuristic approach is studied. Similarly to [9], cost minimization (Capital Expenditures (CapEx) cost normalized to 10G transponder’s cost) is considered as an alternative objective function. The assumption of single-path IP routing is not considered.

Employment of renewable energy sources is considered in [17]. The authors propose an Integer Linear Programming (ILP) and a heuristic called Renewable Energy Optimization hop (REO-hop) targeting minimization of non-renewable energy consumption. Number of multiplexers/demultiplexers, number of fibers on each physical link, number of wavelength channels on each physical and virtual link, number of ports at each node and the multi-path IP routing are kept as variables in the ILP. The REO-hop heuristic is based on the multi-hop bypass heuristic from [9]. Traffic demands are attempted to be routed over the virtual topology so that they traverse the maximum number of nodes using the renewable energy. Should the attempt be unsuccessful, shortest-path routing for the traffic demand is verified. This is in contrast to the multi-hop bypass heuristic, where only the shortest-path routing is verified. Differently from our work, the NSFNET network loaded with random traffic demands is used for the evaluation. Moreover, the IP routing assumption is not varied. The authors of [17] extended their work in [19], where they focused on the physical topology design of IP-over-WDM networks. Variation of the constraints on nodal degree limit and number of links is the main difference from [17]. Furthermore, the authors considered network design for symmetric and asymmetric traffic (hot node scenario), and CapEx minimization.

A 2-step MILP is proposed in [20]. The network at the IP layer is designed first. It is then used as input for the design of the network at the optical layer. The variables include: number of wavelength channels between node pairs on the precomputed K-shortest physical paths, multi-path IP routing, number of fibers on physical links, number of add/drop Dense Wavelength Division Multiplexing (DWDM) ports (connecting a Reconfigurable Optical Add-Drop Multiplexer (ROADM) to an IP router and to other nodes), and number of line cards determining router configuration (S2 fabric cards, Line Card Chassis and Fabric Card Chassis) at each node. The proposed 2-step MILP is evaluated on a small-size network (6 nodes and 8 bidirectional links as in [9]) and the NSFNET (14 nodes and 21 bidirectional links) without comparison against a joint procedure. No heuristic approach is proposed, and no differentiation of IP routing schemes is performed.

The model presented in [21] assumes precomputed routing (corresponding to link-by-link grooming, and end-to-end grooming), and counts the number of necessary devices (routers with line cards, regenerators and fibers with optical amplifiers) according to predefined rules and formulas. No MILP formulation is presented.

None of the works above compare joint and separate solving of the design problem for the IP and WDM layers. The comparison of SPR and MPR is tackled only in [16], but

only using a MILP for a protected backbone network.

### B. IP and WDM Layers Without Fiber Installation

The MILP proposed in [22] finds the IP routing, installed line cards (determining chassis and interconnecting fabrics), LT, and its realization in the WDM layer taking into account physical layer constraints, installed transponders and corresponding slave shelves and racks. The COST239 network (11 nodes and 26 links) is used in this study with the assumption of a single-fiber per link. Heuristic approaches, and variation of IP routing schemes are not considered.

In [10] authors present a model for multi-layer network design. They consider two types of line cards with gray interfaces, diversified lightpath capacities, multiple chassis configurations, and Routing and Wavelength Assignment (RWA). Due to the complexity of the formulated MILP, the problem is optimally solved for a small network (6 nodes and 7 physical links) with one fiber per physical link and 3 wavelengths per fiber. Differently from our work, traffic demands are randomly generated. Similarly to [22], heuristic approaches, variation of IP routing schemes are not considered. CapEx-efficient design is investigated as an alternative optimization objective for the network design.

In [8] the authors focus on two network architectures (IP-over-WDM with gray interfaces and IP-over-Optical Transport Network (OTN)-over-WDM). The optimization model is not explicitly presented, but the authors explain that optimal router basic node and Electrical Cross-Connect (EXC) basic node as well as the degree of the OXC are selected as a result of the optimization. Underlying fiber topology is given (17 nodes and 26 links). No heuristic approaches are investigated and the IP routing is not varied. Power-minimized network is compared against the CapEx-minimized one.

## III. PROBLEM FORMULATION

We model an IP-over-WDM network (Fig. 1) where nodes include both electronic and optical devices. At the WDM layer, OXCs offer optical by-pass technology exploiting optical fibers. OXCs may connect incoming WDM channels to outgoing ones (assuming full wavelength conversion capability), or terminate them in the corresponding nodes equipped with routers in the IP layer. The IP layer is interconnected with the WDM layer by router line cards performing OEO conversion. IP routers can be equipped with several line cards where lightpaths terminate. All parallel lightpaths (regardless of their realization in the WDM layer) between two IP routers form a logical link in the IP layer. A lightpath between two particular line cards may be routed over different physical paths in the WDM layer. The IP traffic demands are routed over the logical links defined by the set of lightpaths.

In the following, we first present the model when adopting the SPR strategy, then the model assuming splittable MCF. Both formulations fall into the class of MILPs problems, which are known to be difficult to solve for medium to large network size. All the notation used in this work is presented in Table I. The MILP formulations are presented for the sake of completeness. Both formulations are also available in [12].

### A. SPR Multi-Layer Problem

Building on the top of the models presented in [4], [23] (and following [12] keeping cost defined as power, and not

as CapEx), let us represent the physical supply network as an undirected graph  $G = (V, E)$ , where  $V$  is the set of nodes where routers can be installed and  $E$  is the set of admissible physical links at which fibers can be installed. Each node  $i \in V$  can be equipped with an IP router  $n$  out of the set  $N$  of IP routers. For each router  $n \in N$ ,  $R^n$  and  $\alpha^n$  are the maximum switching capacity and the associated power consumption, respectively. Let  $\beta^e$  be the power consumption of a fiber (with corresponding OLAs and WDM terminals) installed on physical link  $e \in E$ .  $B$  denotes the capacity of a fiber in terms of wavelength channels. An OXC of infinite capacity is assumed at every physical network node.

Consider now the routing of lightpaths over the physical topology. Let  $P$  be the set of all admissible physical routing paths in  $G$  for all node pairs  $(i, j) \in V \times V, i < j$ .  $P_i \subset P$  is the subset of all admissible physical routing paths ending at node  $i \in V$ .  $P_{(i,j)} \subset P$  is the subset of all admissible routing paths in  $G$  between nodes  $i$  and  $j$  for every node pair  $(i, j) \in V \times V, i < j$ .  $P_e \subset P$  is the subset of all admissible physical routing paths traversing admissible physical link  $e \in E$ . Let us denote by  $C$  the module of bandwidth that can be installed on each path  $p \in P$ . Each module of bandwidth  $C$  on a path  $p$  requires two line cards (one at each end-node of  $p$ ), and uses one wavelength channel on every physical link of the physical routing path. Power consumption of the two line cards is denoted as  $\gamma$ .  $\delta$  denotes the maximum admissible utilization of bandwidth installed on each path  $p \in P$ .  $\delta$  takes values between 0 and 100%. Bandwidth installed on all physical paths  $p \in P_{(i,j)}$  for  $(i, j) \in V \times V, i < j$  forms a logical link between nodes  $i$  and  $j$ . All logical links together with  $V$  constitute the LT.

Let  $d_{ij}$  be the undirected traffic demand value between node  $i$  and node  $j, i < j$ . Let the total demand  $d_i$  of a network node  $i$  be the sum of all traffic demands originating/terminating at  $i$ , i.e.,  $d_i = \sum_{j \in V \setminus \{i\}} (d_{ij} + d_{ji})$ .

We then introduce the model variables. Let  $f_{ij}^{ab}, f_{ji}^{ab}$  be binary variables taking the value 1 if traffic demand between nodes  $a$  and  $b$  uses logical link between nodes  $i$  and  $j$ , 0 otherwise. Let  $y_p \in \mathbb{Z}_+$  be the number of lightpaths realized on  $p \in P$ . Let  $z_e \in \mathbb{Z}_+$  be the number of fibers installed on physical link  $e \in E$ . Finally, let  $x_i^n$  be binary variables set to 1 if router  $n \in N$  is installed at node  $i \in V$ .

We formalize the MILP as (1) with the control variables  $f_{ij}^{ab}, f_{ji}^{ab}, x_i^n \in \{0, 1\}, y_p, z_e \in \mathbb{Z}_+$ .

$$\min \sum_{i \in V, n \in N} \alpha^n x_i^n + \gamma \sum_{p \in P} y_p + \sum_{e \in E} \beta^e z_e \quad (1a)$$

$$\sum_{j \in V \setminus \{i\}} (f_{ij}^{ab} - f_{ji}^{ab}) = \begin{cases} 0 & i \neq a, i \neq b \\ 1 & i = a \\ -1 & i = b \end{cases}, \quad \forall (a, b) \in V \times V, \forall i \in V \quad (1b)$$

$$\sum_{p \in P_{(i,j)}} \delta C y_p - \sum_{a \in V} \sum_{b \in V} d_{ab} (f_{ij}^{ab} + f_{ji}^{ab}) \geq 0, \quad \forall (i, j) \in V \times V \quad (1c)$$

$$\sum_{n \in N} R^n x_i^n - \sum_{p \in P_i} C y_p \geq d_i, \quad \forall i \in V \quad (1d)$$

$$\sum_{n \in N} x_i^n \leq 1, \quad \forall i \in V \quad (1e)$$

$$B z_e - \sum_{p \in P_e} y_p \geq 0, \quad \forall e \in E \quad (1f)$$

TABLE I  
NOTATION USED IN THE MILP, GENETIC ALGORITHM FOR GREEN DESIGN (GAGD), AND METRICS

Symbol	Description	
$G = (V, E)$	undirected physical supply network with the set of nodes $V$ and the set of admissible physical links $E$	
$P$	set of admissible physical routing paths in $G$ for all node pairs $(i, j) \in V \times V, i < j$	
$P_i$	subset of all admissible physical routing paths in $G$ ending at node $i \in V, (P_i \subset P)$	
$P_{(i,j)}$	subset of all admissible routing paths in $G$ between nodes $i$ and $j$ for every node pair $(i, j) \in V \times V, i < j, (P_{(i,j)} \subset P)$	
$P_e$	subset of all admissible physical routing paths traversing admissible physical link $e \in E, (P_e \subset P)$	
$N$	set of IP routers that can be installed in the network	
$R^n$	maximum switching capacity of router $n \in N$	
$\alpha^n$	power consumption of router $n \in N$	
$\beta^e$	power consumption of a fiber (OLAs and WDM terminals) installed on link $e \in E$	
$B$	capacity of a fiber in terms of number of wavelength channels	
$L_e$	length (in km) of the physical link $e \in E$	
$N_a^e$	number of OLAs needed to amplify the signal at edge $e \in E$	
$\beta^a$	power consumption of a single OLA	
$\beta^t$	power consumption of a single WDM terminal	
$\gamma$	power consumption of two line cards	
$C$	module of bandwidth that can be installed on each path $p \in P$	
$\delta$	maximum admissible utilization of bandwidth installed on each path $p \in P$	
$d_{ij}$	undirected traffic demand value between node $i$ and node $j, i < j$	
$d_i$	the total traffic demand of a network node $i$	
$K$	set of commodities corresponding to those nodes in $V$ that are source of at least one demand	
$d_i^k$	net demand value for commodity $k \in K$ and node $i \in V$	
$\Delta$	maximum number of generations without improvements (GAGD)	
$\Theta$	size of the population (GAGD)	
$\Gamma$	size of the offspring (GAGD)	
<hr/>		
Variables	$f_{ij}^{ab}, f_{ji}^{ab}$	whether or not the traffic demand between nodes $a \in V$ and $b \in V$ uses logical link between nodes $i \in V$ and $j \in V$ (both directions), $f_{ij}^{ab}, f_{ji}^{ab} \in \{0, 1\}$ , SPR formulation
	$y_p$	number of lightpaths realized on $p \in P, y_p \in \mathbb{Z}_+$
	$z_e$	number of fibers installed on physical link $e \in E, z_e \in \mathbb{Z}_+$
	$x_i^n$	whether or not router $n \in N$ is installed at node $i \in V, x_i^n \in \{0, 1\}$
	$f_{ij}^k, f_{ji}^k$	the amount of traffic originated at node $a \in V$ and targeted to node $b \in V$ traversing logical link between nodes $i \in V$ and $j \in V$ (both directions), $f_{ij}^k, f_{ji}^k \in \mathbb{R}_+$ , splittable MCF formulation (MPR)
<hr/>		
Metrics	$L^{MPR}$	number of lightpaths in the splittable MCF solution (MPR)
	$L^{SPR}$	number of lightpaths in the SPR solution
	$P^{MPR}$	total power consumption of the splittable MCF solution (MPR)
	$P^{SPR}$	total power consumption of the SPR solution
	$P^{2S}$	total power consumption of a network designed with the two-step procedure
	$P^J$	total power consumption of a network designed with the joint procedure
	$\Delta_L^{SPR-MPR}$	relative increase of the number of lightpaths in the SPR solution w.r.t. the splittable MCF solution (MPR)
$\Delta_P^{SPR-MPR}$	relative increase of the power consumption in the SPR solution w.r.t. the splittable MCF solution (MPR)	
$\Delta_P^{2S-J}$	relative increase of the power consumption due to the two-step procedure w.r.t the joint procedure	

The objective (1a) is to minimize the network total power consumption. The constraints (1b) ensure flow conservation, and enforce single-path routing of the traffic demands over the LT. The constraints (1c) guarantee enough bandwidth on the admissible physical routing paths to accommodate the traffic. Logical node capacity constraints are imposed by (1d), i.e., the capacity of a node is higher or equal to the bandwidth of the attached lightpaths plus the traffic demand generated at the node. The constraints (1e) select a single configuration for each router at each node. The constraints (1f) limit the number of wavelengths used at each fiber.

### B. Splittable MCF Multi-Layer Problem

Following our previous work [12] we need to make the following changes to (1) to design a network under the splittable flows assumption. We introduce the set of commodities  $K$  based on point-to-point demands  $d_{ij}, (i, j) \in V \times V, i < j$ . The set  $K \subseteq V$  corresponds to those nodes in  $V$  that are source of at least one demand. For commodity  $k \in K$  and every node  $i \in V$  we define the net demand value

$$d_i^k = \begin{cases} \sum_{j \in V} d_{ij} & \text{for } i = k \\ -d_{ki} & \text{otherwise} \end{cases} \quad (2)$$

With this definition we subsume all demands whose source is  $k \in V$ . It holds that

$$\sum_{i \in V} d_i^k = 0 \quad (3)$$

for all  $k \in K$ . Notice that the total demand value  $d_i$  of a network node  $i$  can be expressed as

$$d_i = \sum_{k \in K} |d_i^k|. \quad (4)$$

The introduction of commodities reduces the number of variables and constraints from the order  $\mathcal{O}(|V|^4)$  and  $\mathcal{O}(|V|^3)$  to  $\mathcal{O}(|V|^3)$  and  $\mathcal{O}(|V|^2)$ , respectively.

To ensure splittable flows, the flow variables must reflect the actual flow of the commodities between a given node pair. Therefore, we replace the  $f_{ij}^{ab}, f_{ji}^{ab} \in \{0, 1\}$  with  $f_{ij}^k, f_{ji}^k \in \mathbb{R}_+$ . Consequently, the constraints (1b) and (1c) need to be changed accordingly to

$$\sum_{j \in V \setminus \{i\}} (f_{ij}^k - f_{ji}^k) = d_i^k, \quad \forall i \in V, \forall k \in K \quad (5)$$

and

$$\sum_{p \in P(i,j)} \delta C y_p - \sum_{k \in K} (f_{ij}^k + f_{ji}^k) \geq 0, \quad \forall (i,j) \in V \times V, \quad (6)$$

respectively.

The complete MILP with splittable MCF can be found in [4] with  $\delta$  equal to 1.0.

#### IV. GENETIC ALGORITHM FOR GREEN DESIGN

The MILP can be solved for networks of limited size (about 15-20 nodes) in a reasonable amount of time. For larger networks, the MILP can hardly find solutions close to the optimal one in an acceptable time (experiments on a network with 22 nodes provided results with optimization gaps exceeding 20%). Thus, we developed an algorithm named Genetic Algorithm for Green Design (GAGD) to solve the design problem up to medium-sized networks in a reasonable amount of time.

The GAGD is a meta-heuristic inspired by the principles of natural evolution (genetic algorithm). The algorithm adopts an iterative search (evolution process) through a large set of possible solutions (population of individuals) to optimize a specific target (fitness function).

The fundamental elements of a genetic algorithm are the notions of the individual and of the fitness function. The individual is a codified solution of the problem that is tackled, while the fitness function is the optimization target of the problem. In GAGD an individual codifies a possible solution of the network design problem, i.e., an array in which each element indicates the number of lightpaths to be established and the number of fibers to be installed between each pair of nodes. Furthermore, the fitness function is the network power consumption as computed in the objective (1a). Thus, the individual with the lowest value of the fitness function represents the least power-consuming network design.

The main steps of the GAGD are summarized in the pseudo-code of Alg. 1. The input parameters required include network parameters  $NetPar$ , power consumption parameters  $PowerPar$  and parameters to setup the algorithm behavior  $AlgoPar$ . More precisely,  $NetPar$  includes the Traffic Matrix (TM), the physical supply network  $G$ , the bandwidth capacity of a line card  $C$ , the maximum utilization of the

installed bandwidth  $\delta$ , and the number of wavelengths per fiber  $B$ . The GAGD does not require  $P$  (the set of all feasible physical routing paths) as input, because it checks that the path used by a lightpath is admissible (based on its length in km). Furthermore,  $PowerPar$  includes the power consumption of the line cards  $\gamma$ , the power consumption  $\alpha^n$  for router of type  $n$ , for each  $n \in N$ , and the power  $\beta^e$  consumed by a fiber installed on physical link  $e$ , for each  $e \in E$ . Finally, the algorithm parameters  $AlgoPar$  are the maximum number of generations without improvements  $\Delta$ , the size of the population  $\Theta$  and the size of the offspring  $\Gamma$ , where  $\Theta > \Gamma$ . The output of the GAGD is the network design  $netDesign$ : the LT and the number of fibers  $z_e$  installed for any link  $e \in E$ . The LT indicates which lightpaths have to be established and which router type has to be installed at each node of the network. In  $netDesign$  the routing of IP traffic demands in the lightpaths and the routing of the lightpaths over the physical topology are included.

---

#### Algorithm 1 Pseudo-code of the GAGD

---

**Require:**  $NetPar, PowerPar, AlgoPar$

**Ensure:**  $netDesign$

```

1: population=generateFirstPopulation( $NetPar, \Theta$ );
2:  $i=0$ ;
3: fitness=evaluateFitness(population,  $PowerPar$ );
4: while ( $i \leq \Delta$ ) do
5:   offspring=generateOffspring(population,  $\Gamma, NetPar$ );
6:   population=selectPopulation(population, offspring,  $\Theta$ );
7:   newFitness=evaluateFitness(population,  $PowerPar$ );
8:   if (newFitness  $\geq$  fitness) then
9:      $i++$ ;
10:  else
11:     $i=0$ ;
12:    fitness=newFitness;
13:  end if
14: end while
15:  $netDesign=selectDesign(population)$ ;

```

---

The evolution process (i.e., the iterative search) starts from a set of  $\Theta$  randomly generated individuals. The set of these individuals represents the first population (line 1). After the initialization and the evaluation of the fitness function for the individuals of the first population (line 3), the evolution process begins. At each generation (i.e., an iteration of the process) the reproduction phase occurs and the offspring of the current population is created (line 5). In this phase,  $\Gamma$  new individuals are generated. Each new individual is obtained by combining two individuals that belong to the old population. Before accepting the new individual, its feasibility is verified (i.e., check if it satisfies all the constraints introduced in the MILP). If any constraint is violated, the individual is discarded, otherwise it is added to the offspring of the current population.

A new population is selected at the end of the reproduction phase (line 6). The new population is composed of the  $\Gamma$  individuals of the offspring and by the best  $(\Theta - \Gamma)$  individuals of the old population. Then, the fitness function of the new population is computed (line 7) and the fitness value is compared with the minimum one and eventually stored (lines 8 – 13). The evolution process is terminated when the fitness function of the best individual of the population has not improved for  $\Delta$  number of generations (line 4). In this

case, we assume that the GAGD has reached its steady state and the network design, represented by the individual with the lowest fitness function, is selected (line 15).

### A. Joint and Two-Step Design Procedures

The network design problem involves two steps: i) selection of the lightpaths to be established (i.e., design of the LT), and ii) routing of the lightpaths over the physical topology and dimensioning of the number of fibers to be installed. These two steps are usually solved *separately* due to complexity reasons [24], while in our MILP and in the GAGD these two design steps are *jointly* solved. Another reason to prefer the traditional two step procedure (named hereafter the two-step design procedure in contrast to the joint design procedure) is that the LT is usually defined by an Internet Service Provider (ISP) that may be a different entity w.r.t. the owner of the physical infrastructure that performs the design at the WDM layer. Furthermore, the operator may need to modify the LT several times to adapt to the changes of traffic, while it is difficult to change the design of the physical layer after the required infrastructure has been deployed. Finally, an important difference between the two design procedures is that the two-step design minimizes separately the power consumption of the IP and of the WDM equipment, while the joint procedure globally minimizes the power consumption across the layers. Thus, the latter may potentially find a lower power-consuming network design.

We solve the two-step design using two heuristics derived from the GAGD. We split the GAGD into the GAGD-IP and in GAGD-WDM heuristics, which solve the network design, respectively, for the IP and for the WDM layer. Both the heuristics mimic the same steps of the GAGD described in Alg. 1. Clearly, minor differences w.r.t. the GAGD are present in their implementation. In particular, in the GAGD-IP the individual is just the LT, while the fitness function is the power consumption of the IP equipment. The heuristic simply considers the constraints related to the IP layer, the only information required about the physical layer is the existence of at least one feasible path between each pair of nodes. In the case that no admissible path exists for a given pair of nodes, the lightpaths between these nodes cannot be established. The routing of the lightpaths over the physical topology, and thus the check if the employed path satisfies the maximum length, is performed in the GAGD-WDM heuristic. Similarly, in the GAGD-WDM heuristic the individual represents the number of fibers to be installed, while the fitness function is the power consumption of the WDM layer. As a consequence, the considered constraints are related only to the WDM layer that basically consists of ensuring that the lightpaths are correctly routed over paths shorter than 3000 km and that on each physical link the installed fibers can sustain the required capacity.

### B. Complexity Analysis of the GAGD

The GAGD has a computational complexity that mainly depends on the basic characteristics of the evolution process, which are the size of the individual, the size of the population  $\Theta$ , the size of the offspring  $\Gamma$ , and the maximum number of generations without improvement of the fitness function  $\Delta$ .

The most significant element from the complexity perspective is the individual which has size proportional to the number of nodes in the network. In details, the individual



Fig. 2. (Color online) Physical supply topology of the Abilene network.

of the joint GAGD has size  $2 \cdot |V|^2$ , while in both GAGD-IP and GAGD-WDM algorithms the size of the individual is  $|V|^2$ . The size of the individual of the joint GAGD is double w.r.t. the size of individuals of other algorithms, because in the former the individual has to represent the set of lightpaths established among the nodes and also the set of fibers installed, while in the other algorithms the individual has just to represent one of the two sets.

The population size  $\Theta$  and the offspring size  $\Gamma$  are also important because these two parameters define the search space over which the algorithms operate. The larger the values of these parameters are, the larger the search space is, and therefore the number of operations of the evolution process. The value of  $\Delta$  is also influencing the complexity, because it determines for how long the GAGD has to be run. Moreover, the complexity has to take into account the computation of the paths and the checks of the constraints introduced in the MILP formulations, these operations can be done in time  $\mathcal{O}(|V|^2)$ .

Thus, the asymptotic complexity for GAGD, GAGD-IP, and GAGD-WDM algorithms is equal to  $\mathcal{O}(\Delta \cdot \Gamma \cdot \Theta \cdot |V|^2)$ . The complexity of the GAGD differs of a constant factor of 2 (i.e., due to the individual size) which can be neglected in the computation of the asymptotic complexity, but it results in an increased computational requirement for the simulations.

## V. SCENARIO DESCRIPTION

We describe first the considered networks and the corresponding traffic matrices, and later the power model used to obtain performance results.

### A. Networks and Traffic

We examine five different physical supply networks. Three are research and educational networks taken from [25], i.e. the Abilene (Fig. 2), the Germany17 (Fig. 3) and the Géant (see [4]). This choice is dictated by the availability of traffic data in [25]. The other two physical supply networks were defined in the TREND (Towards Real Energy-efficient Network Design) project [26], as forecasts for the year 2020. Topologies and traffic matrices were provided by France Telecom (FT) and Telefónica Investigación y Desarrollo (TID) [27], [28].

1) *Research and Education Networks*: The Abilene topology consists of 12 nodes and 15 physical supply links. The Germany17 topology is composed of 17 nodes and 26 physical supply links, resulting in a larger average nodal degree (3.06)



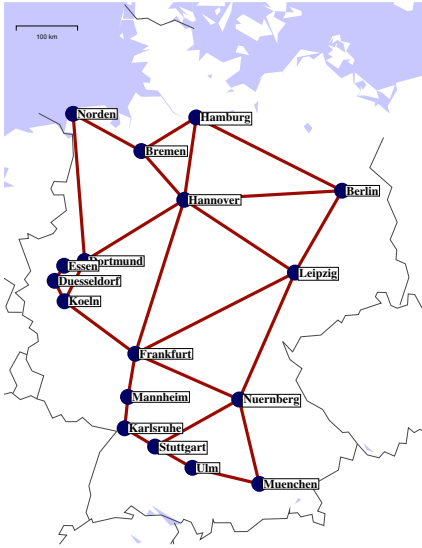


Fig. 3. (Color online) Physical supply topology of the Germany17 network.

than the Abilene topology (2.5). The Géant topology is the largest one from [25], i.e. 22 nodes and 36 physical supply links resulting in an average nodal degree equal to 3.27. Similarly to [4], the set  $P_{(i,j)}$  of paths for potential lightpaths between every node pair  $(i, j) \in V \times V$  was precomputed for each network. The total length of each physical path was limited to 3000 km using the spherical distance for physical link lengths. This corresponds to 72 physical paths for Abilene, 6533 paths for Germany17, and 2970 paths for Géant used by the MILP when solving the network design.

To define the TM, we take the maximum matrix among those available in a given period for each network (between 2004-07-01 and 2004-07-31 for Abilene, 2004-01 and 2004-12 for Germany17, 2005-05-05 and 2005-06-04 for Géant). The available time granularities of the original TMs from [25] are 5 min., 15 min, and 1 month for Abilene, Géant, and Germany17, respectively. The original TMs are rescaled to obtain traffic volumes compatible with today's carried traffic. More precisely, we consider three different traffic levels by scaling up the original TMs so that the total demand per node ( $\sum_{i<j} d_{ij}/|V|$ ), measured in Gigabits per second per node (Gpn), is equal to 100, 300 and 500 Gpn, respectively.

2) *National Operational Networks*: The networks defined by FT and TID comprise more nodes than the ones taken from [25]. The FT physical supply topology consists of 46 nodes and 76 links, while the TID physical supply topology consists of 33 nodes and 53 links [28], with an average nodal degrees equal to 3.3 and 3.2, respectively. More details about the FT and TID scenarios can be found in [27], [28]. Traffic data is envisioned by FT and TID according to three forecasted traffic levels named Low Load (LL), Medium Load (ML), and High Load (HL). The total demand per node (LL/ML/HL) is (472/728/1108) Gpn for FT and (1594/2232/3125) Gpn for TID.

### B. Power Model

The power model is based on power values collected in [7], [29]. In the IP layer, we assume a line card (4-port WDMPHY Physical Layer Interface Module (PLIM) + Modular Services

Card (MSC)) providing capacity  $C$  equal to 40 Gbps and consuming  $\gamma/2$  equal to 500 W. Two line cards are needed for a bidirectional lightpath.

Each node  $N$  is designed on the basis of a set of router configurations, consisting of different number of Line Card Shelves (LCSs) and Fabric Card Shelves (FCSs) without any line cards installed. At most 72 LCSs can be used in a configuration [7]. However, since in some scenarios we forecast traffic for the year 2020, we require router configurations with a larger number of LCSs w.r.t. this limit to satisfy the expected traffic requests.

The power consumption of router of configuration type  $n$  is computed according to the following model:

$$\alpha^n = \mathcal{P}_{LCS} \cdot LCS^n + \mathcal{P}_{FCS} \cdot FCS^n, \quad (7)$$

where  $LCS^n$  and  $FCS^n$  are, respectively, the number of LCSs and of FCSs employed in the router of type  $n$ , while the power consumed by an LCS is equal to  $\mathcal{P}_{LCS} = 2920 W$  and the power consumption of a FCS is  $\mathcal{P}_{FCS} = 9100 W$  according to [7].

The number of LCSs in router of type  $n$  is computed as  $R^n/640$ , where 640 [Gbps] represents the switching capability of a single LCS, while the number of required FCSs interconnecting multiple LCSs can be computed as  $\lceil LCS^n/9 \rceil$  [7]. In the following, we refer to the router of type  $n$  with maximum switching capacity  $R^n$  with the label SH-IP- $R^n$ .

OLAs and WDM terminals contribute to power consumed in the WDM layer. We assume OLAs spanning up to 80 km. Power consumption of Dynamic Gain Equalizers (DGEs) and Dispersion Compensating Fibers (DCFs) (together with the part related to the pre-installed OXC) is neglected due to small power consumption and passive character, respectively. Hence, the total power consumption of each fiber installed on a physical link  $e \in E$  is given by:

$$\beta^e = N_a^e \cdot \beta^a + 2 \cdot \beta^t, \quad (8)$$

where  $N_a^e = \lfloor L_e/80 \rfloor$  is the number of OLAs needed to amplify the signal at edge  $e \in E$  given the physical link length  $L_e$  in kilometers.  $\beta^a$  is the power consumption of a single OLA, and  $\beta^t$  is the power consumption of a single WDM terminal. A WDM terminal is needed at both ends of the fiber.

Since different power values are available in the literature for  $\beta^a$  and  $\beta^t$  (see [7], [29] for an overview), we select two pairs of values (see Table II), corresponding to (i) the reference values from Table 4 of [29], and to (ii) high values from Tables 8 and 9 of [7]. Thus, we cover a realistic range of power consumption of WDM devices.

## VI. RESULTS

To summarize the analyzed scenarios and parameter range, we consider two computation methods (MILP and GAGD), two routing policies (SPR and MPR), five physical networks (Abilene and Germany17 for MILP and GAGD, and Géant, FT and TID for the GAGD) with the corresponding TMs, two values of maximum admissible utilization  $\delta$  (0.5 and 1.0), two pairs of power consumption figures of an OLA and a WDM terminal ((i)  $\beta^a = 110 W, \beta^t = 240 W$ , (ii)  $\beta^a = 622 W, \beta^t = 811 W$ ). Three traffic levels are considered corresponding to Low Load (LL), Medium Load (ML), and High Load (HL). In the case of FT and TID networks the

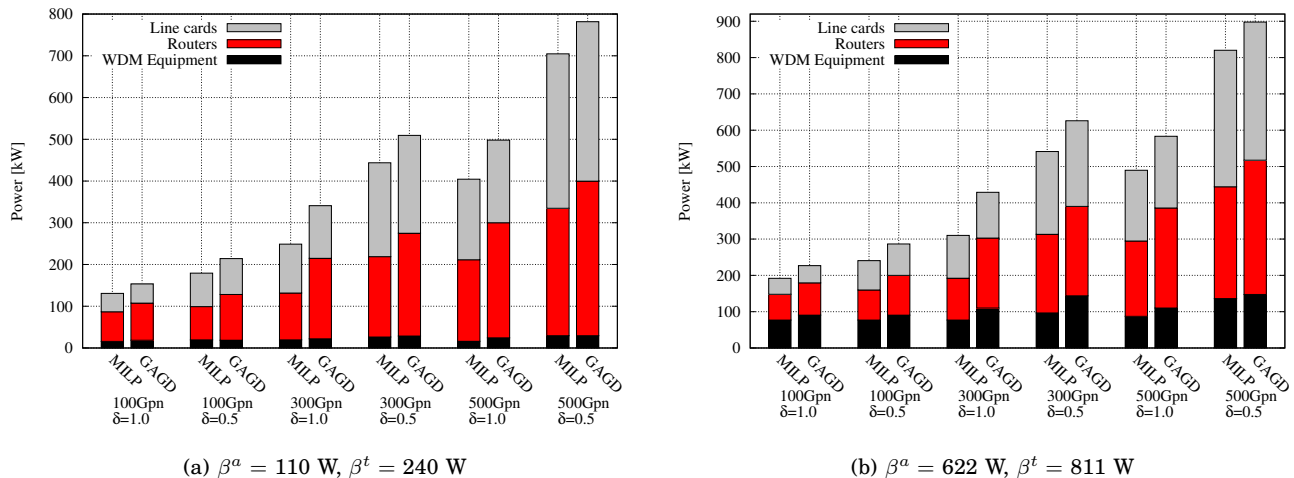


Fig. 4. (Color online) Breakdown of power consumption for the Abilene network.

TABLE II  
POWER CONSUMPTION VALUES OF OPTICAL COMPONENTS AND OF LINE CARDS [7], [29]

SYMBOL	TYPE	DETAILS	Power [W]
$\gamma/2$	IP/Multiprotocol Label Switching (MPLS) Router Line Card	40 Gbps capacity, colored, up to 3000 km reach	500
$\beta^a$	Optical Line Amplifier (OLA)	ELH (80 km span)	(i) 110, (ii) 622
$\beta^t$	WDM Terminals (multiplexer/demultiplexer + booster/receiver amplifier)	80 channel, (Long Haul (LH), Extended Long Haul (ELH), Ultra Long Haul (ULH))	(i) 240, (ii) 811

traffic levels are based on forecasted data. For the Abilene, Germany17, and Géant networks, instead, the traffic levels are based on traffic data originating from measurements. This data has been scaled so that the total demand per node equals 100, 300 and 500 Gpn, which correspond to LL, ML, and HL, respectively. Finally, for the GAGD, we consider two design procedures (joint and two-step) and power consumption as objective (1a).

All the optimization problems were solved using CPLEX [30] installed on a high performance cluster [31] composed of 128 Central Processing Unit (CPU) cores with 568 GB of total memory. The time limit was set to 24 hours for SPR optimization problems, and to 2 hours for MPR problems. The GAGD simulations were instead run on a server equipped with 2 Quad CPU at 2.66 GHz and 4 GB of RAM.

All Abilene splittable MCF problems solutions were very close to the optimal value (gap lower than 1%). The gap exceeded 6% only for three SPR instances (max. 9%). Results for the Germany17 network showed larger gaps. One splittable MCF instance reached a gap of 10.37%, the others being under 6.08%. Gaps in the range 6.75-29.73% were reached for the SPR instances on the Germany17 network.

For the GAGD *AlgoPar*, the population size  $\Theta$  is set to 30, the number of new individuals generated at each iteration  $\Gamma$  to 20, the maximum number of generations without improvements  $\Delta$  to 50 for Abilene, Germany17, and Géant, and to 10 for TID and FT. A sensitivity analysis on these parameters showed a negligible effect on the results.

Unless otherwise stated, in the analysis of results we focus on the SPR policy, the most common routing assumption, and on joint design procedure of GAGD with the objective of power minimization.

#### A. Power Consumption in IP and WDM layers

Fig. 4(a) reports the power consumption of network components, considering  $\beta^a = 110$  W and  $\beta^t = 240$  W in the Abilene network. Results obtained with both the MILP and the GAGD are reported. As expected, the total power consumption raises for increasing traffic, because more devices need to be deployed to satisfy traffic demands. However, the power consumption increase is slower than the traffic increase. The maximum admissible utilization  $\delta$  also plays a crucial role for the network power consumption. For the 300 Gpn case, the total power consumption is 443.79 kW for the MILP with  $\delta = 0.5$ , with a percentage increase of 44% w.r.t. the power consumed with  $\delta = 1.0$ .

Fig. 4(a) also shows the breakdown of power consumption over network components. The largest amount of power consumption is due to routers and line cards rather than WDM equipment. Moreover, while the power consumption of WDM equipment presents only minor increase with the load increase, the total power consumption with the MILP moves from 130.83 kW with 100 Gpn and  $\delta = 1.0$  to 704.72 kW with 500 Gpn and  $\delta = 0.5$ . This suggests that traffic requirements should be carefully estimated when deploying the network to avoid large over-provisioning and large waste of energy consumption. Power consumed by line cards is comparable to the power consumed by router chassis, which indicates high potential of power saving when deploying sleep modes [4]. Finally, the figure reports the results obtained with the GAGD, which, interestingly, is able to find a solution which requires at most 25% of additional power w.r.t. the MILP. This power increase is mainly due to the different types of routers chosen by the GAGD, which consume more power w.r.t the ones selected by the MILP. Indeed, the GAGD is conceived for a directed traffic scenario, while the MILP is



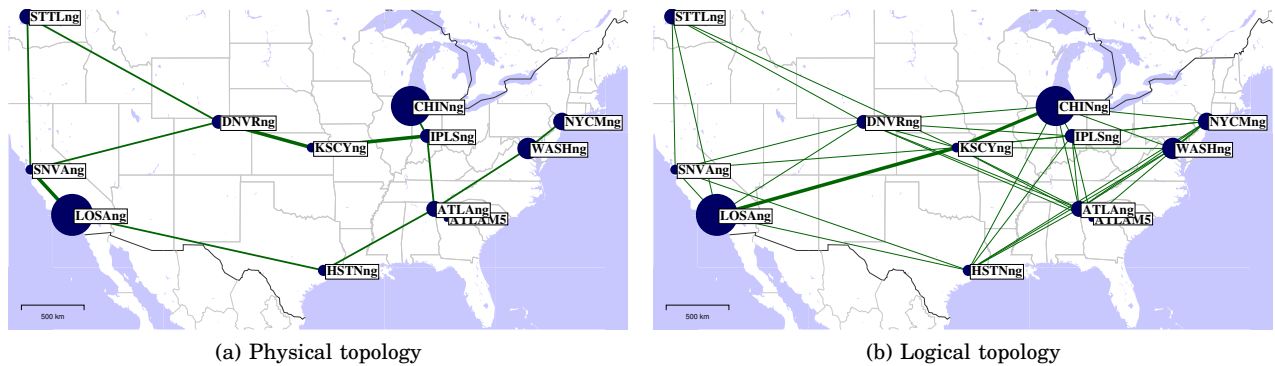


Fig. 5. (Color online) Physical and logical topologies of the Abilene network designed with the MILP, 300 Gpn,  $\delta = 0.5$ ,  $\beta^a = 622$  W, and  $\beta^t = 811$  W.

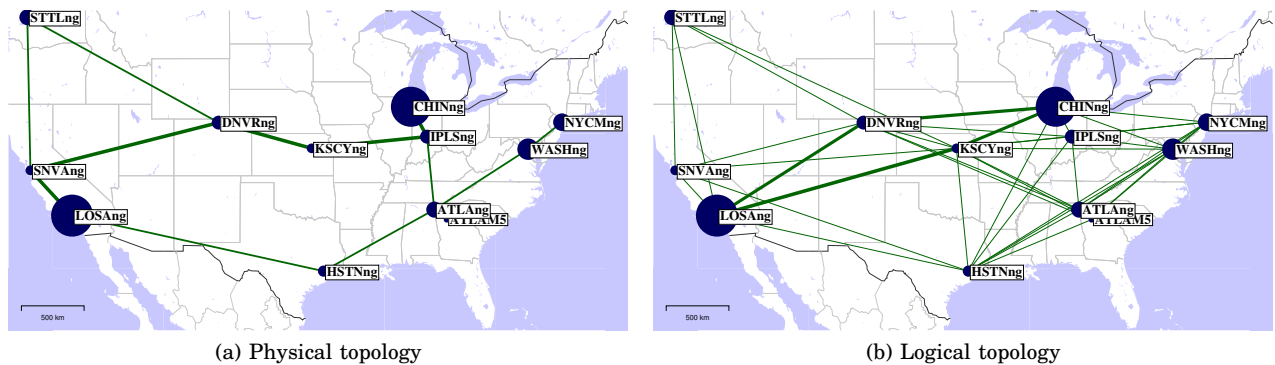


Fig. 6. (Color online) Physical and logical topologies of the Abilene network designed with the GAGD, 300 Gpn,  $\delta = 0.5$ ,  $\beta^a = 622$  W, and  $\beta^t = 811$  W.

formulated for undirected traffic demands, to decrease its complexity. Thus, the GAGD can find a network design in which the number of incoming and outgoing lightpaths is different at each node. As a consequence, the number of line cards that routers are required to host is equal to the maximum between the incoming and outgoing lightpaths. This results in an over-dimensioning of the router capacity w.r.t. the MILP case, and, thus in a larger power consumption.

Fig. 4(b) reports the results with  $\beta^a = 622$  W and  $\beta^t = 811$  W. The power consumption of WDM equipment is still much lower than the consumption of the IP layer at high loads. At low loads, the physical topology becomes a tree, and fibers need to be installed to guarantee connectivity in the WDM layer. While devices of smaller capacity are installed at the IP layer, the fibers and WDM equipment remain underutilized, consuming power comparable to routers and line cards. MILP and GAGD provide similar results.

Fig. 5 reports a graphical visualization of the physical and logical topologies obtained with the MILP for the Abilene network under medium load of 300 Gpn, with  $\delta = 0.5$ ,  $\beta^a = 622$  W, and  $\beta^t = 811$  W. The size of the nodes correspond to the amount of traffic demand generated by each node, while the line thickness is proportional to either the maximum number of installed fibers on a physical link, or lightpaths between a pair of logical nodes. The physical topology evolves with increasing load from a tree to a mesh. For the scenario shown in Fig. 5(a) the physical topology uses 13 physical links out of the 15 possible ones, and the resulting topology is similar to the original supply network of Fig. 2. On the contrary, the LT (Fig. 5(b)) is quite different from the physical one, since many direct lightpaths (bypassing intermediate IP

routers) are preferably deployed. Moreover, several parallel lightpaths are installed between Chicago and Los Angeles, since a large amount of traffic is exchanged between these two cities. Note that there is no direct logical link between Chicago and Los Angeles because the distance between these nodes exceeds the maximum length of a lightpath (3000 km).

In Fig. 6 we report the physical and logical topologies obtained with the GAGD. The physical topology is almost the same as the one obtained with the MILP, apart for more fibers needed on the links between Sunnyvale and Denver and between Chicago and Indianapolis. The additional fiber capacity is required due to the slightly different LT (Fig. 6(b)) w.r.t. the LT of the MILP (Fig. 5(b)). Indeed, several lightpaths are established by GAGD along the path Chicago-Denver-Los Angeles, because traffic demands are considered as directed traffic relations with the same demand value in both directions. More precisely, the traffic from Chicago to Los Angeles is served with a two-hop path having as intermediate node Denver, while the traffic from Los Angeles to Chicago follows a path via Kansas City as intermediate node.

We then consider the Germany17 network. Fig. 7 reports the results obtained considering the different power consumption values for OLAs and WDM terminals. In both cases, the GAGD requires at most 30% of additional power w.r.t. the MILP, and this gap is mainly due to the additional power required by routers. Moreover, the total power consumption of the network is comparable with the Abilene network. For example, with  $\beta^a = 622$  W,  $\beta^t = 811$  W, 500 Gpn and  $\delta = 0.5$  the Germany17 network consumes about 800 kW with the MILP, similarly to the Abilene network. However,

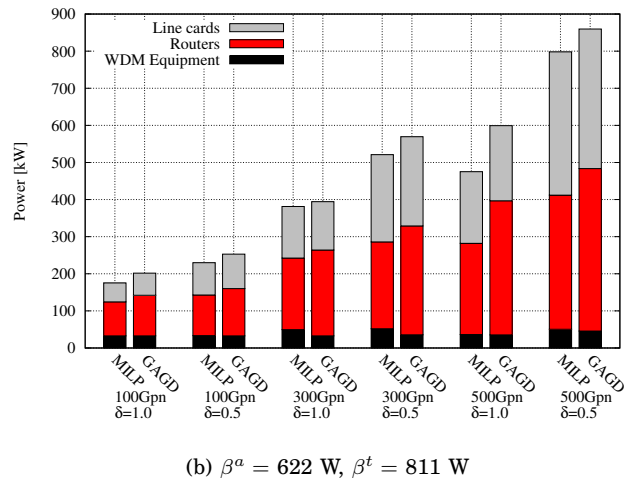
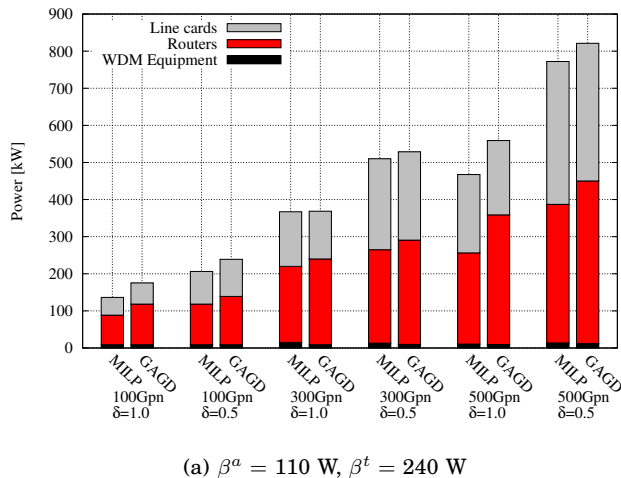


Fig. 7. (Color online) Breakdown of power consumption for the Germany17 network.

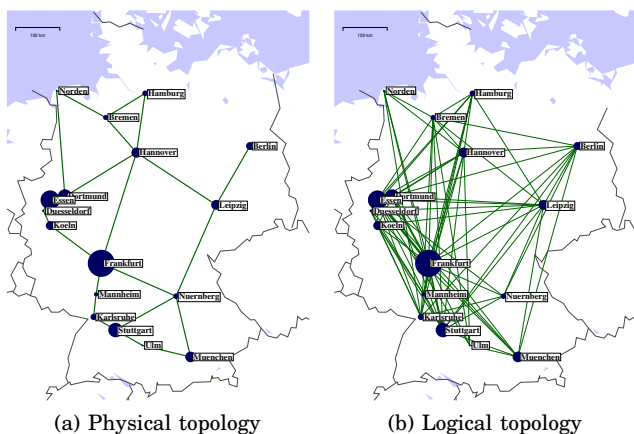


Fig. 8. (Color online) Physical and logical topologies of the Germany17 network designed with the MILP, 300 Gpn,  $\delta = 0.5$ ,  $\beta^a = 622$  W, and  $\beta^t = 811$  W.

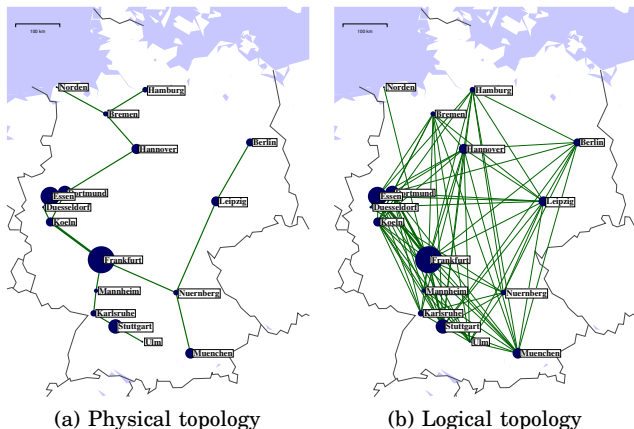


Fig. 9. (Color online) Physical and logical topologies of the Germany17 network designed with the GAGD, 300 Gpn,  $\delta = 0.5$ ,  $\beta^a = 622$  W, and  $\beta^t = 811$  W.

the power share of fibers is lower than in the Abilene case, since the physical links of Germany17 are much shorter, and require fewer OLAs. The power consumption of line cards and routers, on the other hand, is bigger in the Germany17 case. To better explain this issue, Fig. 8 reports the physical

and logical topology obtained with the MILP with 300 Gpn,  $\delta = 0.5$ ,  $\beta^a = 622$  W, and  $\beta^t = 811$  W. The physical topology (Fig. 8(a)) uses 22 physical links out of the 26 available ones. The LT is highly meshed especially at the Frankfurt node (see Fig. 8(b)), since a lot of traffic is originated from and targeted to it. Concentration of traffic at one node results in a need for routers of high capacities (and high power consumption), as discussed next.

The physical and logical topologies for Germany17 designed with the GAGD are shown in Fig. 9. The GAGD finds a physical topology (Fig. 9(a)) with a lower number of used physical links w.r.t. the MILP. Indeed, the power consumption of the WDM equipment is slightly lower than in the MILP solution. However, the total power consumption of the network (objective (1a)) designed with the MILP is lower, because the MILP chooses a LT that consumes a significantly lower amount of power w.r.t. the LT found by the GAGD.

Finally, Fig. 10 reports the power breakdown of the FT network designed with the GAGD. Similar results for Géant and TID are not reported due to lack of space. The total power consumption is consistently higher for the FT network w.r.t. the Abilene and Germany17 networks. Indeed, the FT scenario is targeted for the year 2020, assuming higher values of traffic w.r.t. the current ones. Moreover, the topology has a larger number of nodes (46) and physical supply links (76). However, despite this traffic increase, the power breakdown is very similar to the one of the two other scenarios, being routers and line cards the largest power consumers.

In summary, the largest power consumption is due to line cards and routers for the considered scenarios, even when using high power consumption for OLAs. The proposed GAGD heuristic efficiently approximates the MILP results.

### B. Router Breakdown

We investigate the type of routers that are installed in the network, starting from Abilene. Fig. 11(a) reports the breakdown of routers considering the MILP and the GAGD. Interestingly, many low capacity (and consequently low powered) routers are installed (mostly SH-IP-640). Then, higher capacity devices are used as traffic increases and  $\delta$  decreases. However, low capacity devices are still used, with SH-IP-640 and SH-IP-1280 representing 50% of installed devices

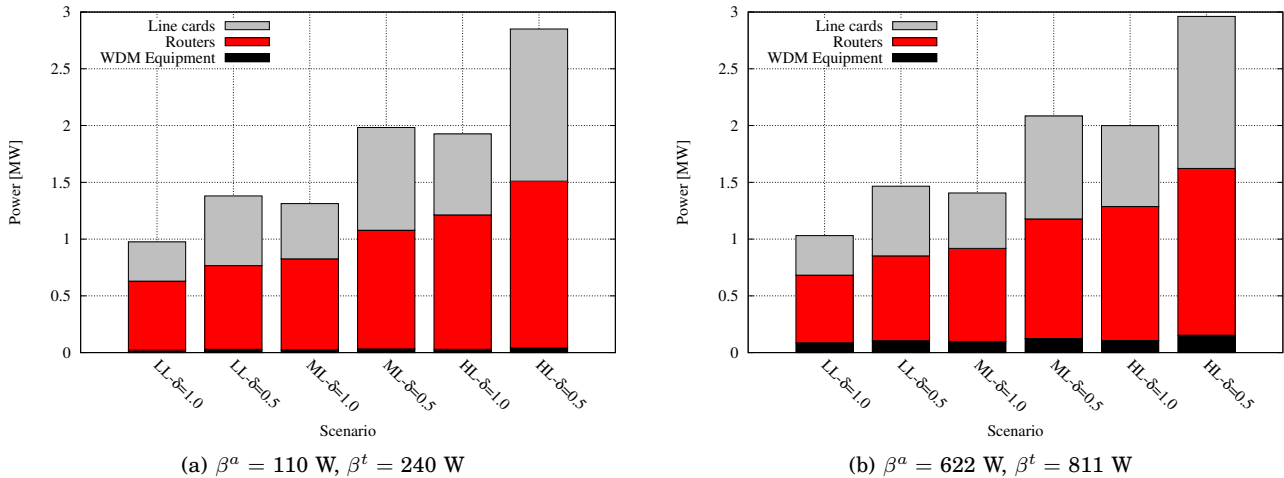


Fig. 10. (Color online) Breakdown of power consumption for the FT network designed with the GAGD.

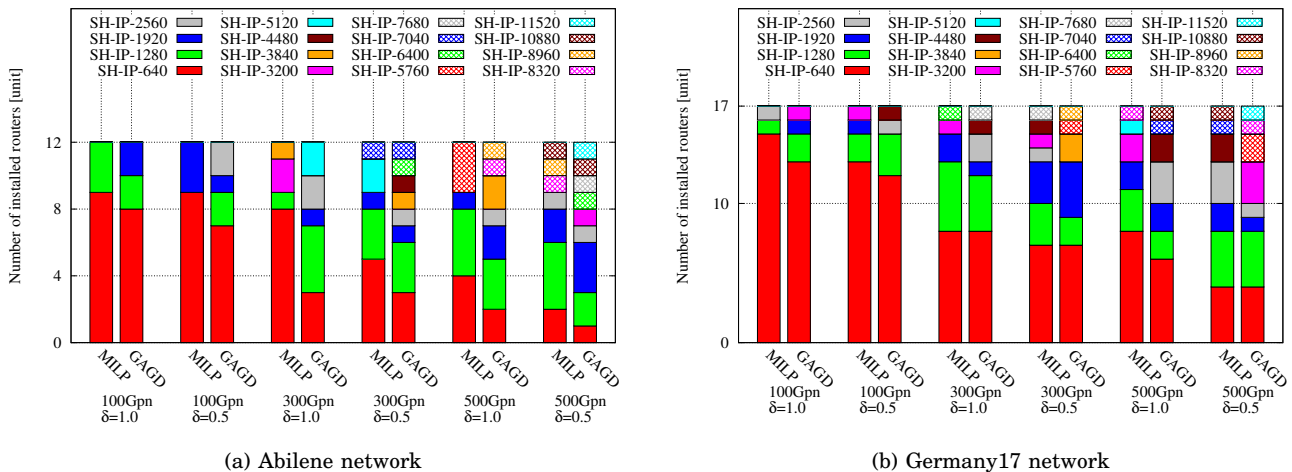


Fig. 11. (Color online) Installed routers (ordered by ascending capacity and power consumption) for MILP and GAGD in Abilene and Germany17 networks.

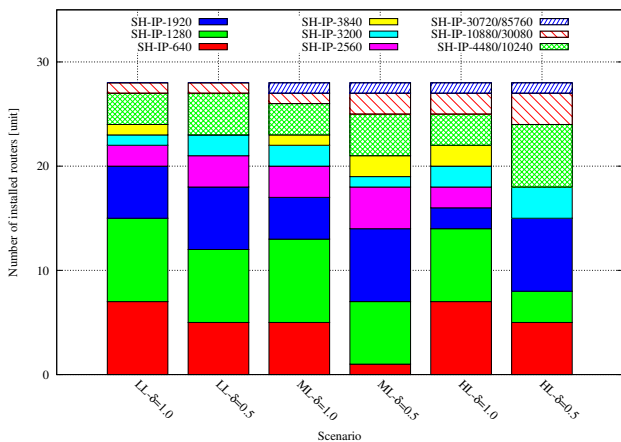


Fig. 12. (Color online) Installed routers (ordered by ascending capacity and power consumption) for GAGD in FT network.

with the MILP even with 500 Gpn and  $\delta = 0.5$ . Focusing on the GAGD, the chosen LTs require to install routers with larger capacities. Thus, more power-hungry routers are used

compared to the MILP and a wider set of installed router types is used.

We then consider the Germany17 network, reported in Fig. 11(b). Differently from the Abilene case, the set of installed routers is more diversified due to the high concentration of traffic in Frankfurt.

Finally, Fig. 12 reports the results obtained with the GAGD over the FT network. The high amount of traffic exchanged in this network imposes the usage of a wide set of devices even for low loads (left part of the figure), and the most power-hungry devices are used for high loads (right part of the figure). The higher capacity routers are grouped in sets for sake of picture's clarity: in each of these groups routers have capacity within the range reported in the legend. Moreover, the number of installed routers is smaller than 46, that is the number of nodes of FT network. Indeed some nodes of the FT network are neither source nor destination of traffic. Therefore no routers need to be installed at these nodes.

In summary, the amount of traffic and its spatial distribution strongly influence the set of installed devices. Moreover, the GAGD tends to use a more diversified set of devices than the MILP.

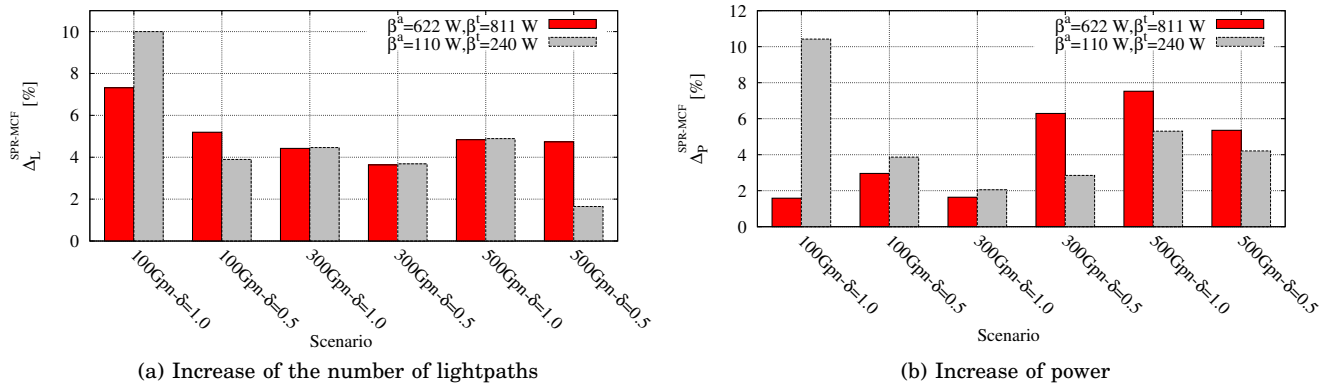


Fig. 13. (Color online) Comparison of networks designed with the MILP constraints for the Abilene network (gap between SPR and MPR).

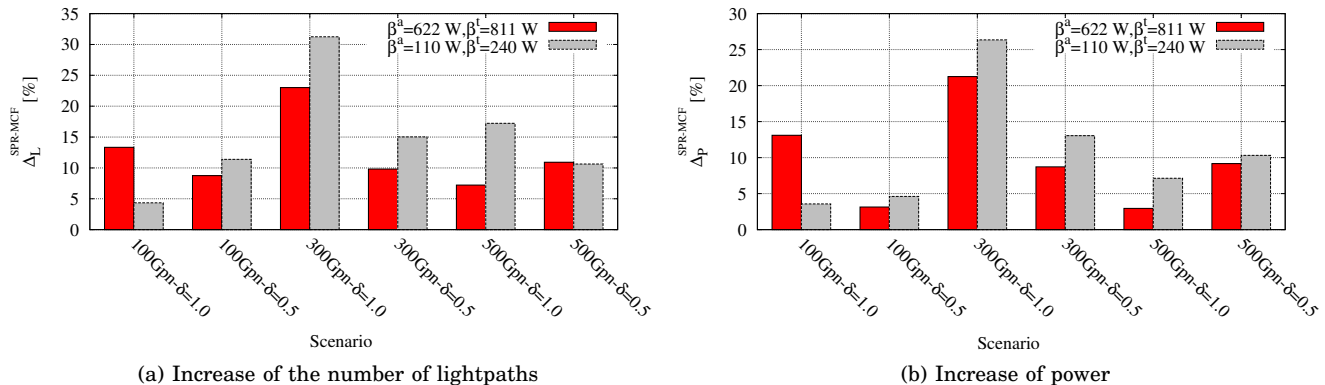


Fig. 14. (Color online) Comparison of networks designed with the MILP for the Germany17 network (gap between SPR and MPR).

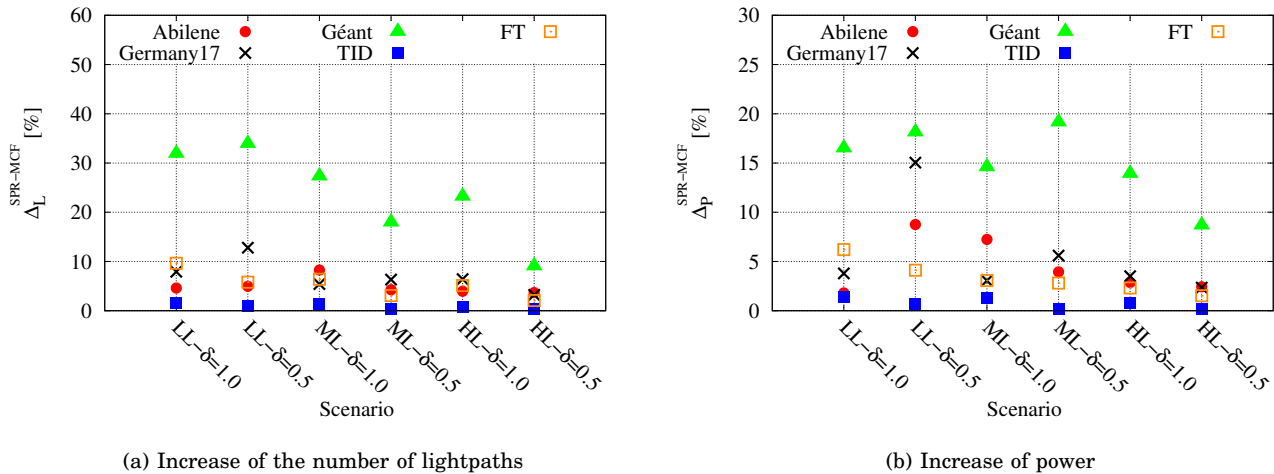


Fig. 15. (Color online) Comparison of networks designed with GAGD (gap between SPR and MPR) with  $\beta^a = 110$  W, and  $\beta^t = 240$  W.

### C. Routing Strategy Impact on Power Consumption

We consider the impact of routing on the total power consumption comparing the SPR results with the MPR ones. Clearly, the splittable MCF problem (Section III-B) is a relaxation of the more realistic SPR (Section III-A), because it adopts fluid routing that can be taken as a lower bound for power consumption. Thus, we expect worse performance when adopting SPR strategy w.r.t. MPR. To capture this effect, we introduce two metrics: the relative increase of the number of lightpaths  $\Delta_L^{SPR-MPR}$ , and the relative increase of power consumption  $\Delta_P^{SPR-MPR}$ . Both metrics are

expressed in percent w.r.t. the network designed using MPR. We define the number of lightpaths obtained solving MPR and SPR as  $L^{MPR}$  and  $L^{SPR}$ , respectively. Then, we define  $\Delta_L^{SPR-MPR}$  as:

$$\Delta_L^{SPR-MPR} = \frac{L^{SPR} - L^{MPR}}{L^{MPR}} \cdot 100. \quad (9)$$

Similarly, we define the total power consumption  $P^{MPR}$  and  $P^{SPR}$ , and the relative increase of power consumption  $\Delta_P^{SPR-MPR}$  as:

$$\Delta_P^{SPR-MPR} = \frac{P^{SPR} - P^{MPR}}{P^{MPR}} \cdot 100. \quad (10)$$

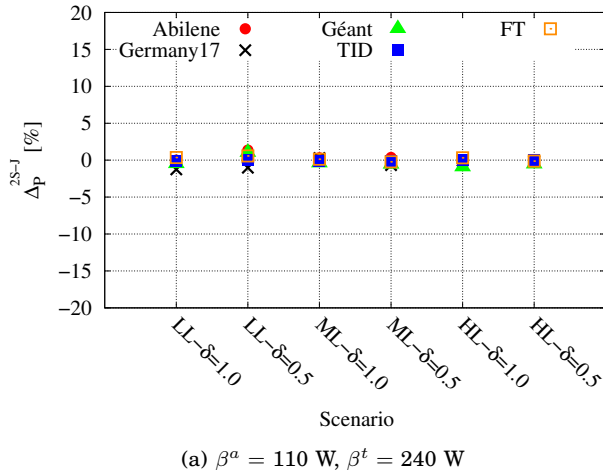
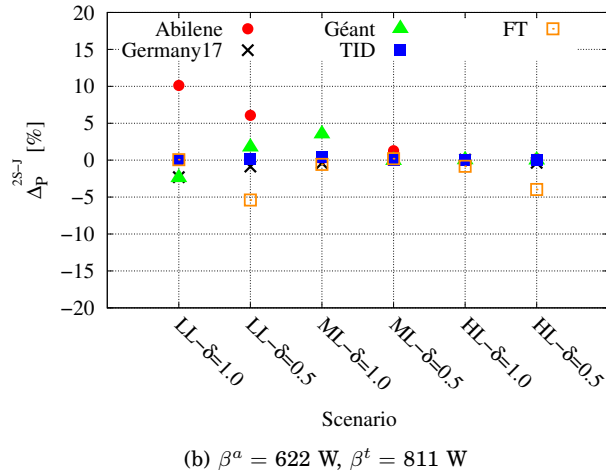
(a)  $\beta^a = 110$  W,  $\beta^t = 240$  W(b)  $\beta^a = 622$  W,  $\beta^t = 811$  W

Fig. 16. (Color online) two-step vs. joint GAGD Comparison.

Fig. 13 reports the results obtained with the MILP for the Abilene network, plotting  $\Delta_L^{SPR-MPR}$  (Fig. 13(a)) and  $\Delta_P^{SPR-MPR}$  (Fig. 13(b)). Interestingly,  $\Delta_L^{SPR-MPR}$  never exceeds 10%, with a decreasing trend for the scenarios in which more capacity is required. This suggests that the number of lightpaths is very similar for both MPR and SPR. Furthermore,  $\Delta_P^{SPR-MPR}$  is lower than 11% for all cases, suggesting that adopting SPR marginally impacts the power consumption.

We also compare the MILP results obtained with MPR and SPR over the Germany17 network, as reported in Fig. 14. Differently from the Abilene case, the adoption of the SPR strategy has a large impact on  $\Delta_L^{SPR-MPR}$ , requiring even more than 30% of additional lightpaths w.r.t the MPR case (Fig. 14(a)). However, power consumption using SPR is at most 26.5% higher than when using MPR (Fig. 14(b)).

In Fig. 15, we report  $\Delta_P^{SPR-MPR}$  and  $\Delta_L^{SPR-MPR}$  computed with the GAGD for all the considered networks. Similarly to the MILP results, all values of  $\Delta_P^{SPR-MPR}$  are within the 20%, with Géant being the network with the largest impact on the power consumption. In other words, the adoption of MPR does not significantly reduce the network power consumption. Finally,  $\Delta_L^{SPR-MPR}$  is following the same behavior of  $\Delta_P^{SPR-MPR}$  with higher values. This confirms that the power consumption is mainly due to line cards and routers, whose total power consumption is proportional to the number of established lightpaths.

Summarizing, the introduction of realistic constraints, namely, the SPR policy, increases the power consumption and the number of lightpaths, but not significantly.

#### D. Two-step Versus Joint Design Procedures

Now we explore two network design procedures, two-step and joint, as described in Section IV-A. The joint procedure minimizes the power consumed by the IP and the WDM layer, as in objective (1a), while in the two-step procedure the design and the minimization is performed independently per layer. Thus, the joint procedure should bring higher power reductions.

The results for the joint design procedure are obtained using the GAGD assuming MPR. Results obtained with SPR routing policy are similar and they are not shown due to space limitation. We define with  $P^{2S}$  and  $P^J$  the total

power consumption of a network designed, respectively, with the two-step and the joint procedures. The power increase obtained by solving the design when using the two-step procedure w.r.t the joint procedure is defined as:

$$\Delta_P^{2S-J} = \frac{P^{2S} - P^J}{P^J} \cdot 100. \quad (11)$$

Fig. 16(a) and Fig. 16(b) report the power increase percentage for two power scenarios. For almost all the considered traffic and networks the two procedures find either similar network configurations or different configurations but with similar power consumption. However, in some cases the two-step procedure is able to find better results. Indeed, the joint procedure, if optimally solved with the MILPs, would always find a result equal or better than the two-step procedure. However, in this case, results are retrieved using a meta-heuristic (i.e., the GAGD) for complexity reasons. Thus, these results are not optimal and it is possible that in some cases the two-step procedure provides slightly better results than those of the joint one due to the sub-optimality of the heuristics. Several factors, such as the simulation run, the traffic matrices, or the physical supply topologies of the networks, can have different impact on the results obtained with the two procedures, and may lead the two-step procedure to achieve better results. However, in most of the cases, the joint procedure is achieving, as intuitively expected, equal or better results than the two-step one.

The two-step procedure usually returns slightly worse results than the joint procedure, but the difference is not significant. Furthermore, the designer of the logical and of the physical topology are different entities, typically the former is an ISP while the latter is the owner of the physical infrastructure. Thus, the design is usually performed separately. According to these considerations, we conclude by suggesting that the two-step procedure should be preferred.

## VII. CONCLUSIONS

We investigated the problem of power-efficient design of IP-over-WDM networks, explicitly targeting the power consumption minimization. We formulated the problem as a MILP, and we proposed GAGD, a genetic algorithm that can scale up to medium-sized networks. Performance results obtained over an extensive set of network scenarios and



parameter values indicate that both the MILP and the GAGD provide power-efficient networks. The total power consumption when adopting SPR is at most 26.5% higher than when assuming splittable MCF. Furthermore, most of the power in an IP-over-WDM network is consumed by routers and line cards, even when high power consumption of OLAs and WDM terminals are assumed.

We also found that the GAGD requires at most 30% of additional power w.r.t the optimal solution. We compared the two-step versus the joint version of the algorithm, showing that the two-step version should be preferred, because it provides networks with similar power consumption and it allows each ISP to design its own LT and the owner of the physical infrastructure to design the WDM layer.

As future research activities, we plan to study the design problem adopting next generation devices, whose power consumption will be more proportional to load. Finally, we want to assess how the introduction of sleep mode capabilities in the IP layer influences the design phase.

#### ACKNOWLEDGMENT

The research leading to these results has received funding from the European Union Seventh Framework Programme (FP7/2007-2013) under grant agreement n. 257740 (Network of Excellence “TREND”).

#### REFERENCES

- [1] M. Pickavet, W. Vereecken, S. Demeyer, P. Audenaert, B. Vermeulen, C. Davelder, D. Colle, B. Dhoedt, and P. Demeester, “Worldwide energy needs for ict: The rise of power-aware networking,” in *Proc. of the ANTS, Mumbai, India*, December 2008.
- [2] A. P. Bianzino, C. Chaudet, D. Rossi, and J. Rougier, “A Survey of Green Networking Research,” *IEEE Communications Surveys & Tutorials*, vol. 14, no. 1, pp. 3–20, 2012.
- [3] R. Bolla, R. Bruschi, F. Davoli, and F. Cucchietti, “Energy Efficiency in the Future Internet: A Survey of Existing Approaches and Trends in Energy-Aware Fixed Network Infrastructures,” *IEEE Communications Surveys & Tutorials*, vol. 13, no. 2, pp. 223–244, 2011.
- [4] F. Idzikowski, S. Orlowski, C. Raack, H. Woesner, and A. Wolisz, “Dynamic routing at different layers in IP-over-WDM networks – maximizing energy savings,” *Optical Switching and Networking, Special Issue on Green Communications*, vol. 8, no. 3, pp. 181–200, July 2011.
- [5] Y. Zhang, P. Chowdhury, M. Tornatore, and B. Mukherjee, “Energy Efficiency in Telecom Optical Networks,” *IEEE Communications Surveys & Tutorials*, vol. 12, no. 4, pp. 441–458, 2010.
- [6] C. Lange, D. Kosiankowski, C. Gerlach, F.-J. Westphal, and A. Gladisch, “Energy Consumption of Telecommunication Networks,” in *Proc. of the ECOC, Vienna, Austria*, September 2009.
- [7] F. Idzikowski, “Power consumption of network elements in IP over WDM networks,” Technical University of Berlin, Telecommunication Networks Group, Tech. Rep. TKN-09-006, July 2009.
- [8] E. Palkopoulou, D. A. Schupke, and T. Bauschert, “Energy efficiency and CAPEX minimization for backbone network planning: Is there a tradeoff?” in *Proc. of the ANTS, New Delhi, India*, December 2009.
- [9] G. Shen and R. S. Tucker, “Energy-minimized design for IP over WDM networks,” *Journal of Optical Communications and Networking*, vol. 1, no. 1, pp. 176–186, June 2009.
- [10] W. Shen, Y. Tsukishima, K. Yamada, and M. Jinno, “Power-efficient multi-layer traffic networking: Design and evaluation,” in *Proc. of the ONDM, Kyoto, Japan*, February 2010.
- [11] R. Ahuja, T. Magnanti, and J. Orlin, *Network Flows: Theory, Algorithms, and Applications*. Prentice Hall, 1993.
- [12] F. Idzikowski, L. Chiaraviglio, and F. Portoso, “Optimal Design of Green Multi-layer Core Networks,” in *Proc. of the e-Energy, Madrid, Spain*, May 2012.
- [13] A. Bianco, E. Bonetto, and A. Ahmad, “Energy awareness in the design of optical core networks,” in *Proc. of the OFC/NFOEC, Anaheim, USA*, March 2013.
- [14] A. Coiro, M. Listanti, T. Squarcia, A. Valenti, and F. Matera, “Energy-minimised virtual topology design in IP over WDM backbone networks,” *IET Optoelectronics, Special Issue on Green Photonics*, vol. 6, no. 4, pp. 165–172, August 2012.
- [15] A. Tzanakaki, K. Katrinis, T. Politi, A. Stavdas, M. Pickavet, P. Van Daele, D. Simeonidou, M. J. O’Mahony, S. Aleksić, L. Wosinska, and P. Monti, “Dimensioning the Future Pan-European Optical Network With Energy Efficiency Considerations,” *Journal of Optical Communications and Networking*, vol. 3, no. 4, pp. 272–280, April 2011.
- [16] A. Betker, D. Kosiankowski, C. Lange, F. Pfeuffer, C. Raack, and A. Werner, “Energy efficiency in extensive multilayer core and regional networks with protection,” Konrad-Zuse-Zentrum für Informationstechnik Berlin, Tech. Rep. ZR 12-45, 2012.
- [17] X. Dong, T. El-Gorashi, and J. M. H. Elmirghani, “IP over WDM Networks Employing Renewable Energy Sources,” *Journal of Lightwave Technology*, vol. 29, no. 1, pp. 3–14, January 2011.
- [18] P. Chowdhury, M. Tornatore, A. Nag, E. Ip, T. Wang, and B. Mukherjee, “On the Design of Energy-Efficient Mixed-Line-Rate (MLR) Optical Networks,” *Journal of Lightwave Technology*, vol. 30, no. 1, pp. 130–139, January 2012.
- [19] X. Dong, T. El-Gorashi, and J. Elmirghani, “On the energy efficiency of physical topology design for IP over WDM networks,” *Journal of Lightwave Technology*, vol. 30, no. 12, pp. 1931–1942, June 2012.
- [20] L. Wang, R. Lu, Q. Li, X. Zheng, and H. Zhang, “Energy efficient design for multi-shelf IP over WDM networks,” in *Proc. of the INFOCOM Workshop on Green Communications and Networking, Shanghai, China*, April 2011.
- [21] W. Van Heddeghem, M. De Grotte, W. Vereecken, D. Colle, M. Pickavet, and P. Demeester, “Energy-efficiency in telecommunication networks: Link-by-link versus end-to-end grooming,” in *Proc. of the ONDM, Kyoto, Japan*, February 2010.
- [22] G. Rizzelli, A. Morea, M. Tornatore, and O. Rival, “Energy efficient traffic-aware design of on-off multi-layer translucent optical networks,” *Computer Networks*, vol. 56, no. 10, pp. 2443–2455, July 2012.
- [23] S. Orlowski, “Optimal design of survivable multi-layer telecommunication networks,” PhD thesis, Technische Universität Berlin, May 2009.
- [24] R. Ramaswami and K. Sivarajan, “Design of logical topologies for wavelength-routed optical networks,” *Journal on Selected Areas in Communications*, vol. 14, no. 5, pp. 840–851, June 1996.
- [25] sndlib, “Library of test instances for Survivable fixed telecommunication Network Design,” <http://sndlib.zib.de/home.action>, 2011.
- [26] Towards Real Energy-efficient Network Design (TREND), <http://www.fp7-trend.eu>, 2010.
- [27] O. Renaïs and J. L. Briand, “Tracks for transport network architecture optimization,” in *Proc. of the Networks, Rome, Italy*, October 2012.
- [28] F. Idzikowski, E. Bonetto, Ł. Budzisz, L. Chiaraviglio, A. Cianfrani, A. Coiro, R. Duque, W. Van Heddeghem, F. Jiménez, J. López Vizcaíno, F. Matera, I. Monroy, F. Musumeci, A. Pattavina, E. Le Rouzic, A. Valenti, and Y. Ye, “Final report for the IRA Energy-efficient use of network core resources,” TREND Project, Deliverable D3.3, June 2012.
- [29] W. Van Heddeghem, F. Idzikowski, W. Vereecken, D. Colle, M. Pickavet, and P. Demeester, “Power consumption modeling in optical multilayer networks,” *Photonic Network Communications*, vol. 24, no. 2, pp. 86–102, October 2012.
- [30] IBM – ILOG, “Cplex,” <http://www.ilog.com/products/cplex/>, 2009.
- [31] DAUIN - Politecnico di Torino, “HPC Project,” <http://dauin-hpc.polito.it>, 2011.